Munkres, K. O., & Richards, R. M. (1965) *Arch. Biochem. Biophys. 109*, 466–479.
Nelson, J. A., Kahn, S., Spencer, T. A., Sharpless, K. B., & Clayton, R. B. (1976) *Bioorg. Chem. 4*, 363.
Rahimtula, A. D., & Gaylor, J. L. (1972) *J. Biol. Chem. 247*, 9–15.
Rahman, R., Sharpless, K. B., Spencer, T. A., & Clayton, R. B. (1970) *J. Biol. Chem. 245*, 2667–2671.
Resnick, M. A., & Mortimer, R. K. (1966) *J. Bacteriol. 92*, 597–600.
Scheffler, I. E. (1974) *J. Cell. Physiol. 83*, 219–230.
Schlenk, H., & Gellerman, J. L. (1960) *Anal. Chem. 32*, 1412–1414.
Sharpless, K. B., Snyder, T. E., Spencer, T. A., Maheshwari, K. K., Nelson, J. A., & Clayton, R. B. (1968) *J. Am. Chem. Soc. 90*, 6874–6875.
Sharpless, K. B., Snyder, T. E., Spencer, T. A., Maheshwari, K. K., Nelson, J. A., & Clayton, R. B. (1969) *J. Am. Chem. Soc. 91*, 3394–3396.
Steinberg, D., & Avigan, J. (1969) *Methods Enzymol. 15*, 514–522.
Swindell, A. C., & Gaylor, J. L. (1968) *J. Biol. Chem. 243*, 5546–5555.
Wada, F., Hirada, K., & Sakamoto, Y. (1969) *J. Biochem. (Tokyo) 65*, 171–175.
Yamamoto, S., & Bloch, K. (1970) *J. Biol. Chem. 245*, 1670–1674.

Phosphorus-31 Nuclear Magnetic Resonance of Double- and Triple-Helical Nucleic Acids. Phosphorus-31 Chemical Shifts as a Probe of Phosphorus–Oxygen Ester Bond Torsional Angles†

David G. Gorenstein,*‡ Bruce A. Luxon, Evelyn M. Goldfield, Kofen Lai, and Donna Vegeais

ABSTRACT: The temperature dependence to the ^{31}P NMR spectra of poly[d(GC)]·poly[d(GC)], $d(GC)_4$, phenylalanine tRNA (yeast) and mixtures of poly(A) + oligo(U) is presented. The ^{31}P NMR spectra of mixtures of complementary RNA and of the poly d(GC) self-complementary DNA provide torsional information on the phosphate ester conformation in the double, triple, and "Z" helix. The increasing downfield shift with temperature for the single-strand nucleic acids provides a measure of the change in the phosphate ester conformation in the single helix to coil conversion. A separate upfield peak (20–26% of the total phosphates) is observed at lower temperatures in the oligo(U)·poly(A) mixtures which is assigned to the double helix/triple helix. Proton NMR and UV spectra confirm the presence of the multistrand forms. The ^{31}P chemical shift for the double helix/triple helix is 0.2–0.5 ppm upfield from the chemical shift for the single helix which in turn is 1.0 ppm upfield from the chemical shift for the random coil conformation.

We have recently proposed that ^{31}P chemical shifts in phosphate esters may serve as a direct probe of P–O ester bond torsional angles. Both theoretical considerations [Gorenstein & Kar, 1975; see also Gorenstein (1975, 1978, 1981) and Pradd et al. (1979)] and direct experimental tests of this hypothesis [Gorenstein et al., 1976; Gorenstein & Luxon, 1979; see also Patel (1979a,b) and Gueron & Shulman (1975)] confirm that the ^{31}P signal of a phosphate diester monoanion in a gauche,gauche (g,g)[1] conformation (as found in the helix state) should resonate several parts per million upfield from a diester in a nongauche conformation (as found in the random coil state).

These conclusions prove to be especially significant since other spectroscopic probes fail to provide detailed conformational information on the phosphate ester bonds in the nucleic acids. Since it is now believed that of the six torsional angles that largely define the conformational structure of nucleic acids, the two P–O ester torsional angles provide the main conformational flexibility to the nucleic acid backbone (Kim et al., 1973; Sundaralingam, 1969). Thus ^{31}P NMR can monitor the "helix–coil" transitions in single-stranded nucleic acids (Gorenstein et al., 1976; Haasnoot & Altona, 1979). A large (0.7–1.3-ppm) downfield shift for a wide structural range of nucleic acids was observed (Gorenstein et al., 1976) upon raising the temperature. At low temperature the nucleic acids will exist largely in a base stacked, helical conformation with the phosphate ester predominantly in the g,g conformation, while at higher temperatures the nucleic acids will largely exist in random coil, unstacked conformations with the phosphate ester in an increased proportion of nongauche (i.e., g,t, etc.) conformations [see, for example, reviews such as Ts'o (1975)].

Earlier ^{31}P NMR[2] model studies were conducted on a number of simple ribo- and deoxyribodinucleoside monophosphates and homopolyribonucleic acids [see also Akasaka et al. (1975) and Cozzone & Jardetzky (1976)]. In the present work we extend these ^{31}P NMR studies on single-stranded nucleic acids to double- and triple-stranded nucleic acids. In

† From the Department of Chemistry, University of Illinois, Chicago, Illinois 60680. *Received August 18, 1981.* Supported by research grants from the National Institutes of Health, the National Science Foundation, and the Alfred P. Sloan Foundation. Purchase of the Nicolet 1080 Fourier transform data system and the Bruker WP-80 spectrometer was assisted by National Science Foundation Department Equipment Grants. The Purdue Biological NMR facility was supported by the National Institutes of Health (RRO 1077).

‡ Fellow of the Alfred P. Sloan Foundation.

[1] We should mention that for purposes of conveniently describing the torsional dependence to chemical shifts, we generally make no distinction between torsional angles +60° (+g) or −60° (−g). In addition, ω,ω' torsional angles of g,t (60°,180°), $-g,t$, t,g, and $t,-g$ will often be grouped together as g,t. Similarly, g,g includes conformers $-g,-g$, $g,-g$, and $-g,g$, although the latter two conformers do have ^{31}P chemical shifts that are different from g,g (Gorenstein & Kar, 1975).

[2] Abbreviations: NMR, nuclear magnetic resonance; ORD, optical rotatory dispersion; CD, circular dichroism, EDTA, (ethylenedinitrilo)-tetraacetic acid; poly(A), poly(adenylic acid); oligo(U), oligo(uridylic acid); poly[d(GC)], poly(deoxyguanidylcytidylic acid); bp, base pair.

0006-2960/82/0421-0580$01.25/0

particular, separate ^{31}P signals are observed for the multi-stranded poly(A)·oligo(U) helix and the single-strand forms of poly(A) and oligo(U). ^{31}P NMR thus will be shown to provide a useful tool for direct estimation of the fraction of the different strand forms in solution.

Use of poly[d(GC)]·poly[d(GC)] which forms a "Z-DNA" conformation at high salt concentrations (Pohl & Jovin, 1972; Wang et al., 1979; Patel et al., 1979) provides an important model for testing the theoretical predictions of the stereoelectronic (P–O ester bond torsional angle) effect in ^{31}P chemical shifts since in Z-DNA the conformation of the phosphodiester backbone alternates between *g,g* and *g,t*. Finally, these model systems will also serve as a basis for understanding the ^{31}P NMR spectra of more complex nucleic acids (such as the transfer RNAs).

Experimental Procedures

NMR Spectra. All of the nucleic acids were obtained from either Sigma Chemical Co., P-L Biochemials, Boeringer Mannheim, or Collaborative Research. To safeguard against possible contamination of the biochemicals by paramagnetic metal ion impurities, we dissolved all (except the tRNA) in double distilled water and passed them through a column of Chelex-100 ion-exchange resin (Na^+ form) purchased from Bio-Rad Laboratories. The eluent was lyophilized, and the solid was dissolved in buffer solution [12–30 mg/mL for poly(A)·oligo(U) and 50 OD units/0.4 mL for poly[d(GC)]·poly[d(GC)]] if it was to be used immediately or stored at −5 °C if it was to be used at some later time. The pH of the buffer–nucleic acid solutions was adjusted on a Radiometer Model PHM 64 Research meter to a pH of 7.0. The tRNA samples were prepared as previously described (Gorenstein & Luxon, 1979). ^{31}P NMR spectra were recorded on a Bruker WP-80 FT spectrometer at 32.4 MHz or a superconducting Nicolet NTC-360 spectrometer at 145.7 MHz (^{31}P). For the high-field NMR studies, the nucleic acid solution plus 20% D_2O for field locking was placed in a Wilmad spherical microcell which in turn was inserted into a 12 mm OD NMR tube containing distilled water. In the low-field NMR studies, the sample was placed in a 5-mm NMR tube. Sample volume for both high- and low-field spectra was 0.4–0.5 mL.

High-field, Fourier transform ^{31}P NMR spectra were taken on the Nicolet NTC-360 spectrometer with 56° pulses, 16K data points, and a 1.86-s recycle time. At low field, 67–75° pulses, 4K–8K data points, and 2.0-s recycle times were used. Some spectra used 90° pulses and a 4.0-s recycle time. The spectra were broad-band ^{1}H decoupled. The temperature of the sample was controlled to within ±1 °C by Bruker or Nicolet (on the NTC-360 spectrometer) temperature control units with nitrogen gas as a coolant. Decoupling at the superconducting field produced about 10–15 °C heating of the sample above the gas stream measured temperatures, even when using a gated two-level decoupling procedure [see Gorenstein & Luxon (1979)]. A correction of the heating problem is described below.

All chemical shifts were referenced to 15% phosphoric acid in D_2O (0.00 ppm) at room temperature (25 °C). This sample is 0.453 ppm upfield from 85% H_3PO_4 with an external D_2O lock. Positive chemical shifts are downfield from phosphoric acid.

External Standard Measurements. The poly(A) used in an external standard measurement experiment was purified of paramagnetic metal ions by extraction of the aqueous solution with dithiazone (Baker) in CCl_4. After the solution was further washed with CCl_4 to remove remaining dithiazone, the sample was centrifuged and the aqueous layer placed in an NMR tube. An external standard of trimethyl phosphate (0.164 M) in a concentric capillary was inserted into a 5-mm NMR tube containing a 1:1 poly(A)–oligo(U) sample which was 18 mM in base pairs.

NOE Measurements. The nuclear Overhauser effect (NOE) measurements were done on the Bruker WP-80 by using a sample which was 64 mM in base pairs in standard buffer. Measurements used 90° pulses, 4K data points, an 18-s recycle time, and 750 scans. Spectra were alternated between broad-band decoupling and a gated decoupling procedure where the decoupler was off for 14 s between scans and turned on 0.002 s before the 4-s acquisition. These spectra were then Fourier transformed by using 16K of memory, with no exponential multiplication.

^{1}H spectra were taken on the WP-80 FT NMR spectrometer in D_2O buffer.

UV Spectra, Melting Curves, and Mixing Plots. Uv spectra were taken on a Varian/Cary 210 UV/VIS spectrophotometer equipped with the capability for direct plotting of absorbance vs. temperature. Melting curves were obtained by monitoring spectral changes with slow cooling (<0.5 °C/min) of the sample through the melting transition (80–4 °C). Melting temperatures, T_m, represent the midpoint of the transition unless otherwise specified and are little different (±2 °C) from the T_m's defined by the inflection point in the curves. Little hysteresis (±2 °C) in T_m was observed if the same samples were slowly heated through the transition.

Determination of extinction coefficients was done by hydrolyzing the poly(A) or oligo(U) at pH 11.6 for 1 h at 40 °C. The absorbance of the hydrolyzed sample was measured at pH 7 at 260 nm and room temperature [$\epsilon_{260} = (15.4 \pm 0.4) \times 10^3$ for adenosine monophosphate and $\epsilon_{262} = (10.0 \pm 0.4) \times 10^3$ for uridine monophosphate].

^{31}P Thermometer. In order to correct for the solution heating by the decoupler, we designed a ^{31}P "thermometer". A solution of trimethyl phosphate (10 mM), sodium hydrogen phosphate (10 mM), and EDTA (1 mM) in a Tris buffer (100 mM) and in the appropriate salt solution (0.1 M NaCl) in 20% D_2O was adjusted to pH 7.0. The added salt was calculated to yield the approximate total ionic strength of the nucleic acid solution since decoupler heating is greater at higher salt concentrations. The frequency separation between the trimethyl phosphate and inorganic phosphate signals is temperature sensitive (Figure 1). Trimethyl phosphate shifts downfield with increasing temperature while the inorganic phosphate shifts upfield as the pH decreases with increasing temperature (Tris p*K* is very sensitive to temperature). The shift range (1.5 ppm) and reproducibility of the measured shift difference from 0 to 90 °C are sufficient to calibrate the internal temperature of the ^{31}P thermometer to ±1 °C. The same thermometer sample was used on the NTC superconducting and Bruker WP-80 spectrometers. The temperature on the WP-80 spectrometer was directly measured in the probe with a Wilmad 5-mm thermometer. The ^{31}P shift difference (and hence sample temperature) on the Bruker spectrometer was the same with the decoupler off or set to 2.0 W. In contrast, the NTC decoupler heated the sample by 16 °C (at 10 °C) to 4 °C (at 70 °C) even with a two-level decoupling procedure (gated low, 1 W, at all times except during collection of the FID when it was gated high, 2 W). Single-level, 4 W decoupling produced greater than 25 °C heating and points out the importance of correction for this problem at very high fields.

Results

Poly(A)·Oligo(U) UV Spectroscopy. By monitoring the

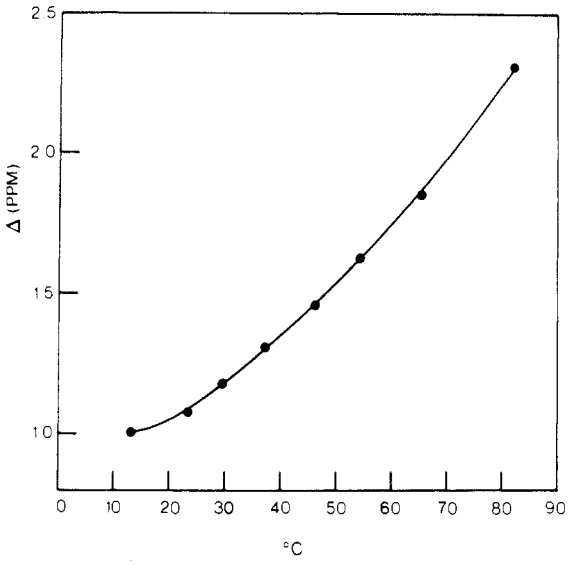

FIGURE 1: ^{31}P thermometer. Chemical shift difference (●) between trimethyl phosphate and phosphate ^{31}P signals as a function of temperature (°C).

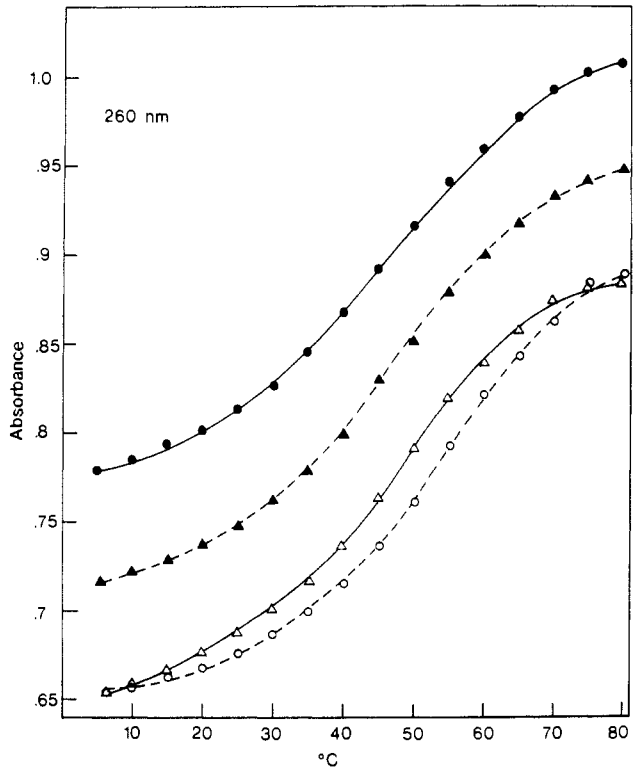

FIGURE 2: Ultraviolet melting curves of 1:1 (▲), 1:2 (△), 1:3 (○), and 2:1 (●) mixtures of poly(A) and U_{20} in 0.2 M NaCl, 10 mM cacodylate, and 1 mM EDTA, pH 7.0.

absorbance at 260 and 280 nm for various mixtures of poly(A) and U_{20} (P-L Biochemicals; average strand length, 20 bases) at constant total nucleotide concentration, we were able to demonstrate the presence of both double and triple helices (data not shown). Thus breaks occurred in the mixing curves at roughly 33 and 50% poly(A) at 5 °C, 280 nm. The absorbance changes at 260 nm monitor melting of double (breaks at 50%) and triple (breaks at 33%) helices, whereas only triple-helix to single-strand equilibria are monitored at 280 nm (Stevens & Felsenfeld, 1964).

Melting curves (Figure 2) at various concentrations, salt conditions, and proportions of poly(A) + oligo(U) confirm that a cooperative melting of these multistrand helices occurs at

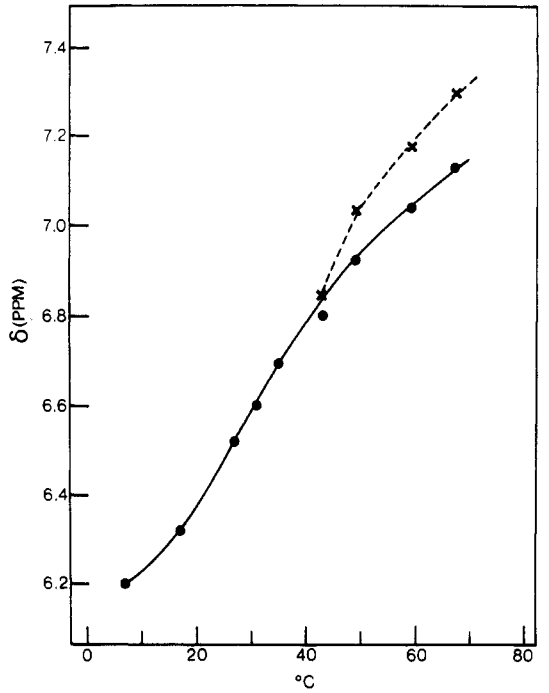

FIGURE 3: Proton NMR chemical shift vs. temperature for the H6 proton in U_7 (●) and the H2 proton of poly(A) (×) in a 1:1 complex in 1 mM EDTA and D_2O.

melting temperatures, T_m, between 45 and 55 °C.

^1H NMR of Poly(A)·Oligo(U). The temperature dependence to the H2 and H6 signals of the adenosine ring in poly(A) and the uracil ring in U_7 (P-L Biochemicals; average strand length, seven bases), respectively, is shown in Figure 3. Assignment of the signals in the high-temperature spectra is based upon the spectral assignments of mononucleotide models (Borer et al., 1975). In this 1:1 mixture, association via base stacking and H bonding in a multistranded complex produces an upfield shift in the H-6 signal (0.8 ppm) (Patel, 1979a,b; Borer et al., 1975). The sigmoidal curve with T_m ~ 30 °C thus monitors melting of the multistranded helices.

The ^{31}P NMR spectra of poly(A)·U_{20} at a 1:1 ratio and a 1:2 ratio are shown in Figures 4–6. At high temperatures the spectra correspond to the superposition of the individual nucleic acid components.

Heterogeneity in the single-strand forms of the nucleic acids is shown by the additional minor ^{31}P signals in these spectra at high temperature. These signals must either represent phosphates in different sections of the strands (middle vs. ends) or in different strand lengths [the poly(A) and oligo(U) samples are only mixtures of various lengths with averages of >400 bases and ~20 bases, respectively). Note that two quite distinct poly(A) single-strand signals (intensity ~2:1) are observed at 145.8 MHz (Figure 5B). In addition, heterogeneity in the oligo(U) sample can be seen most clearly in the ^{31}P spectrum of Figure 4B. This highly resolved spectrum reveals, besides the main oligo(U) downfield signal at 0.11 ppm, additional minor signals at 0.22 ppm and at 0.06 ppm [a downfield shoulder to the poly(A) signal]. This heterogeneity explains why even in the completely relaxed ^{31}P spectrum of Figure 4B, the apparent signal intensities and areas for the two main signals corresponding to oligo(U) and poly(A) are not in the expected ratio of 1:1. Note that sample concentrations were determined by measurement of the optical density at 260 nm of standard solutions of the separate nucleic acids. Mixtures were prepared volumetrically from these standard solutions, and extinction coefficients for the nucleic acids were even redetermined (see Experimental Procedures)

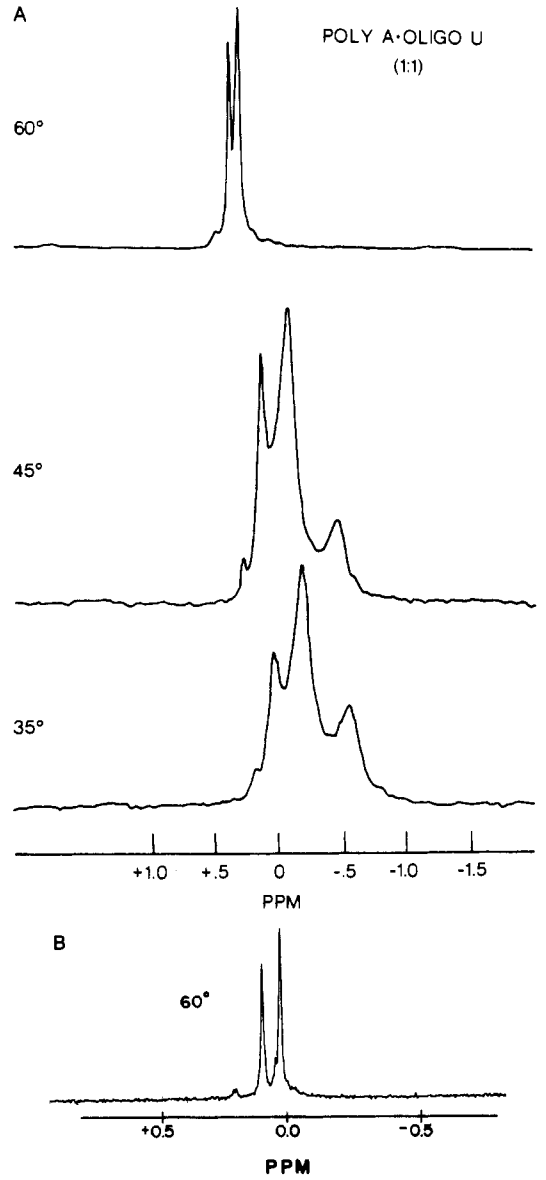

FIGURE 4: ^{31}P NMR spectra for poly(A)·U_{20} (1:1) at various temperatures in 0.2 M NaCl, 10 mM cacodylate, 1 mM EDTA, pH 7.0, and 20% D_2O. (A) 32.4 MHz, total nucleotide concentration was 24 mg/mL, exponential line broadening, 1 hertz, and a 4-s recycle time. (B) Same as (A) but at 60 °C, no exponential line broadening, and a 18-s recycle time.

with a value for poly(A) within 1% of the literature and with a slightly higher value for oligo(U) (9.4×10^3 as opposed to 8.9×10^3). The use of the new extinction coefficients for sample preparation in later experiments did not markedly affect the relative peak intensities. However, including the two minor signals in the oligo(U) integration, the intergrated intensities are within ±2% of the expected 1:1 ratio.

A second reason for the apparent discrepancy between the observed and expected signal intensities at higher temperatures in Figures 4 and 5 lies in the difference between the spin–lattice (T_1) relaxation times of the poly(A) and oligo(U) signals. Since the oligo(U) is a smaller molecule, it will have a longer T_1 than poly(A). The nuclear Overhauser effects of the two main signals are, however, nearly equal: 1.78 ± 0.05 for the oligo(U) signal and 1.76 ± 0.06 for poly(A), at 60 °C (E. Goldfield, unpublished experiments). Using a T_1 of 1.75 s for poly(A) (Akasaka, 1975) and the equality of the NOE's, we have roughly calculated that the T_1 for oligo(U) is 2.8–3.2 s. With a 4-s recycle time and a 90° pulse, the ratio of the oligo(U) main signal to the poly(A) main signal in the 1:1 sample is only 0.68 (spectra not shown). This ratio increases to 0.80 in Figure 4B with a recycle time of 18 s. Both signals are near their equilibrium magnetization with the longer recycle time while with the shorter times the oligo(U) signal is partially saturated relative to the poly(A) signal.

At lower temperatures ($T < T_m \sim 48$ °C) a new broad upfield signal appears 0.4–0.6 ppm upfield from the single-strand nucleic acids. ^{13}P melting curves (Figures 6 and 7) and line-width data (Figure 8) confirm that this upfield signal (above 0.8 ppm) corresponds to the double and/or triple helices.

^{31}P spectra and melting curves for poly[d(GC)]·poly[d(GC)] are shown in Figures 9 and 10, respectively. Besides the phosphate diester signals shown in Figure 9, two smaller monoester signals (total of 15% of total phosphate) are observed between 4 and 5 ppm. This is confirmed by the observation that 16% of the total nucleic acid OD_{260} units are not precipitated in perchloric acid, and thus at most 16% of the sample represents small (<10 bp) oligonucleotides (Cohen et al., 1981). Our sample has either a number of single-strand breaks or a small amount of oligonucleotide fragments. However, this poly[d(GC)] has a reported sedimentation coefficient, $s_{20,w}$, of 8.2 (P-L Biochemicals circular), and UV spectroscopy shows that it does not melt up to 95 °C, confirming that it is indeed a high molecular weight preparation. Thus Cohen et al. (1981) have shown that a sonicated sample of poly[d(GC)] characterized as being 50–200 bp in length has a T_m of 58.5 °C under low salt conditions. $d(GC)_4$ has a T_m of 65 °C under high salt conditions (K. Lai, unpublished experiments). The high melting temperature for this sample, the absence of even any minor transition in the UV melting curve from room temperature to 95 °C, and the absence of any sharp melting transition in the ^{31}P melting curve of Figure 10 suggest that these minor monoester phosphate signals likely originate from very small oligo[d(GC)] fragments (<4 bp) or infrequent single-strand breaks along the chain which will not affect our conclusions.

^{31}P Spectra and Melting Curves for Phenylalanine tRNA. The ^{31}P spectra of yeast phenylalanine tRNA under high Na^+ (ca. 0.2 M total Na^+) and no added Mg^{2+} reveal a number of phosphate diester signals spread over ~7 ppm besides the downfield 3′-phosphate monoester (at +3.0 ppm) (Figure 11). As earlier reported by Gueron & Shulman (1975), Gorenstein & Luxon (1979), Salemink et al. (1979, 1981), and Gorenstein et al. (1981), these ^{31}P spectral changes reflect melting of the secondary and tertiary structure in the L-shaped native structure. It has been suggested earlier that the main upfield signal (M) in the main cluster corresponds to the double-helix diesters in the cloverleaf structure and the downfield signals (J; K) in the main cluster correspond to nonhelical phosphates.

The main cluster upfield signals L and M at −1.0 ppm shift downfield by a total of 0.8–0.9 ppm with increasing temperature. The other main signal at −0.8 ppm also shifts downfield, and the two peaks merge at 70 °C. The shoulder peaks in the main cluster and all of the scattered peaks eventually merge into the single random coil diester peak at high temperature upon melting of the secondary and tertiary structure. Except for U only small shifts are observed for the scattered signals prior to their disappearance at 40–50 °C. The sharp melting of the native tRNA structure in the absence of Mg^{2+} around 50 °C is consistent with ^{1}H NMR (Kan et al., 1977; Robillard et al., 1977) and optical melting (Romer et al., 1977) studies and Gueron & Shulman's (1975) earlier ^{31}P study. In addition, the more recent studies (Gorenstein & Luxon, 1979; Salemink et al., 1979) suggest that the disappearance of the

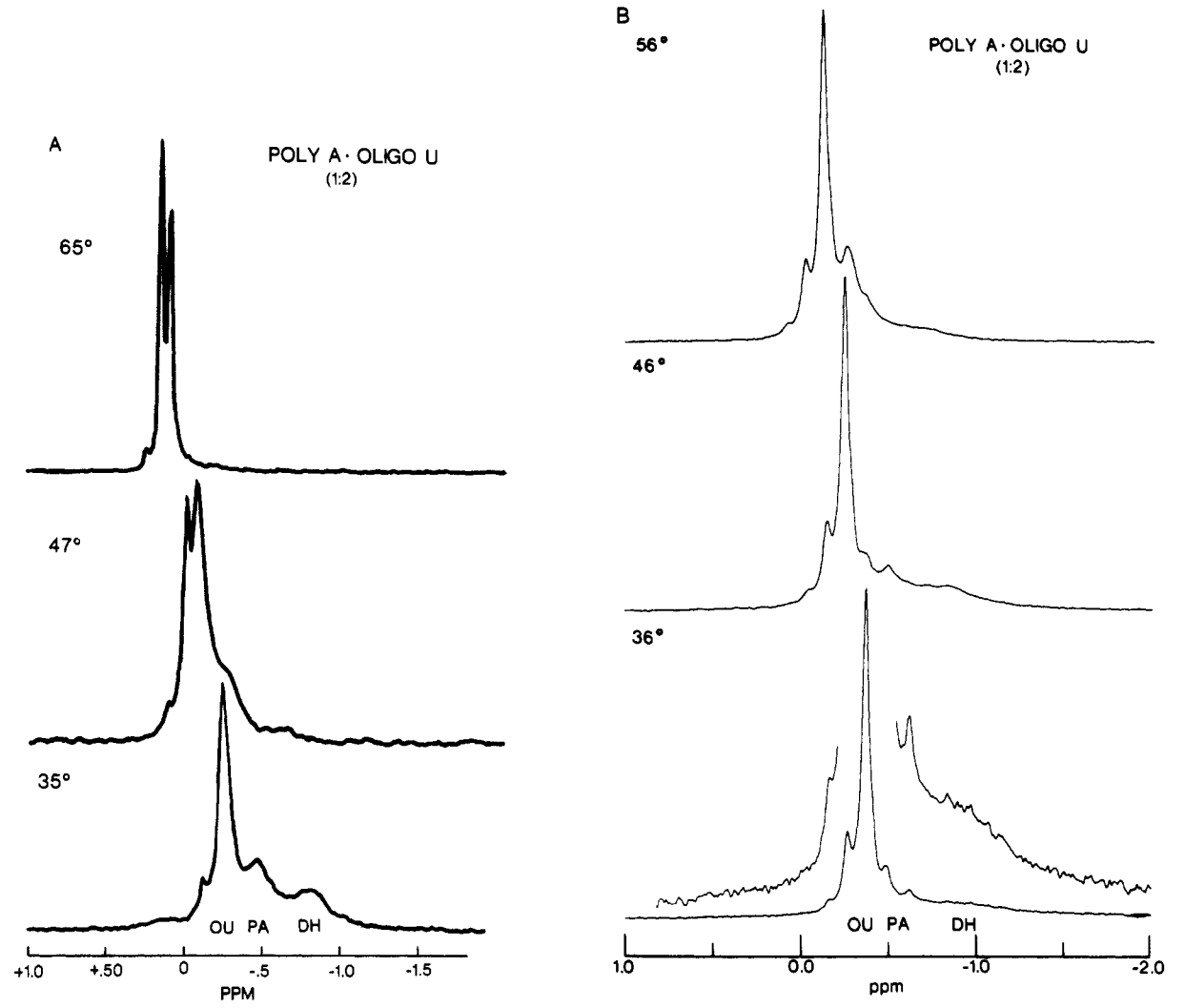

FIGURE 5: ^{31}P NMR spectra for poly(A)·U_{20} (1:2) at various temperatures in 0.2 M NaCl, 10 mM cacodylate, 1 mM EDTA, pH 7.0, and 20% D_2O. (A) 32.4 MHz; total nucleotide concentration was 24 mg/mL. (B) 145.8 MHz; nucleotide concentration was 17 mg/mL.

scattered peaks is associated with loss of tertiary structure.

Discussion

Single-Strand Nucleic Acids. In previous studies (Gorenstein et al., 1976; Gorenstein, 1978) we presented evidence that the 0.7–1.3-ppm downfield shift at elevated temperature of various single-stranded nucleic acids reflected the base stacked, single helix to unstacked, random coil transition. Haasnoot & Altona (1979) have recently confirmed this interpretation as has the work of Patel (1979a,b) and Yamada et al. (1978) on ^{31}P NMR of other model nucleic acids. The phosphate conformation goes from *g,g* (helical) at low temperature to a mixture of *g,g*, *g,t*, *t,t*, etc. conformations in the melted, high-temperature state.

Mixtures of Complementary Nucleic Acids: Double and Triple Helices. The single-stranded nucleic acids are not ideal models for locking a phosphate diester into a *g,g* conformational state since considerable conformational flexibility still exists in the single-stranded, "helical" nucleic acids even at 0 °C (Ts'o, 1975).

The double-helical state is much more limited as to the backbone flexibility, and generally the phosphate diester conformation is limited to *g,g* (Arnott, 1970). The ^{31}P chemical shift of a mixture of complementary nucleic acids will hopefully therefore provide better information on the ^{31}P chemical shift of a *g,g* phosphate diester.

Self-complementary polymers or mixtures of complementary polymers would eliminate this problem since melting temperatures of double-stranded polymers are >50 °C (Bloomfield et al., 1974) and at room temperature exist almost entirely in the double-helix state (*g,g* phosphate diester conformation). Unfortunately, the ^{31}P NMR signal of such a double-helical polymer at lower temperatures is generally too broad to be very useful or even observable (Akasaka et al., 1975; Patel & Canuel, 1976; Hanlon et al., 1976).

Our choice of complementary oligo(U) and poly(A) was intended to avoid this problem since the double-helix state in this mixture will have single-strand breaks every 20 uridine bases, corresponding to the length of the oligo(U) chain based upon M_w ~7500). This imparts considerable flexibility to the polymer·oligomer complex although not as much as present in the single-strand poly(A).

The Multistrand. The assignment of the new upfield (0.8–0.9-ppm) signal to the double-helical (and/or triple-helical) state is suggested by (1) the signal broadness and (2) the sharp transition for its melting.

(1) As shown in Figure 8 the downfield signal we have assigned to oligo(U) stays quite narrow, <5 Hz (at 32.4 MHz), over the temperature range of 25–65 °C. It is only slightly broader (7–8 Hz) at 146 MHz. The poly(A) signal is also only slightly broader at 32 MHz over this temperature range (3–8 Hz) but is substantially broader at 146 MHz (20–30 Hz). The upfield double (triple) helix signal is broader yet. At 32 MHz it is 6–9 Hz while at 146 MHz it increases from 50 to 109 Hz as the temperature is lowered (Figure 8).

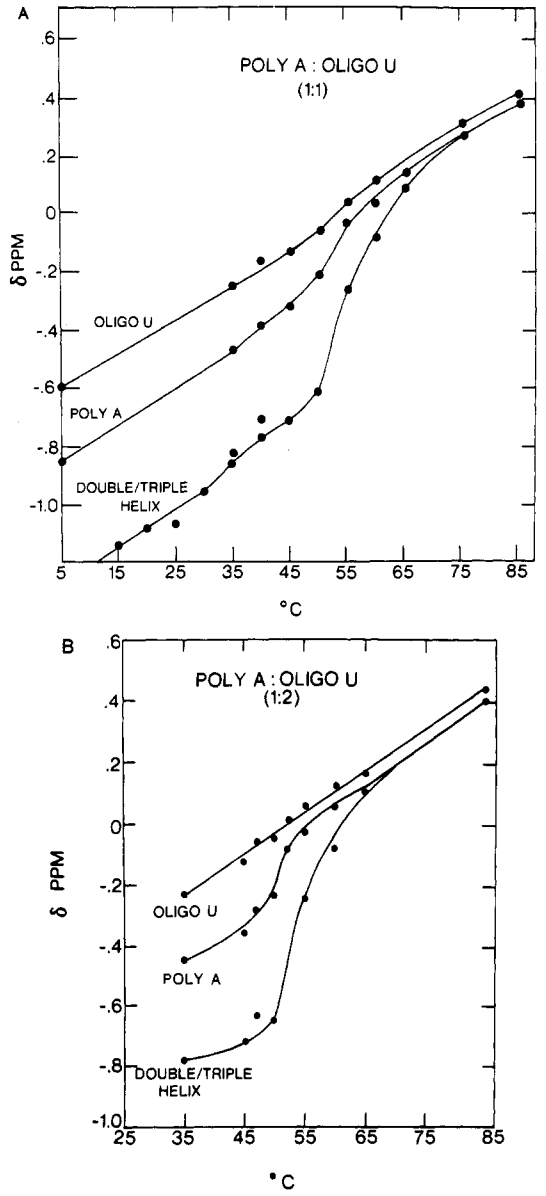

FIGURE 6: ^{31}P chemical shift vs. temperature for spectra of Figure 4A (A) and Figure 5A (B).

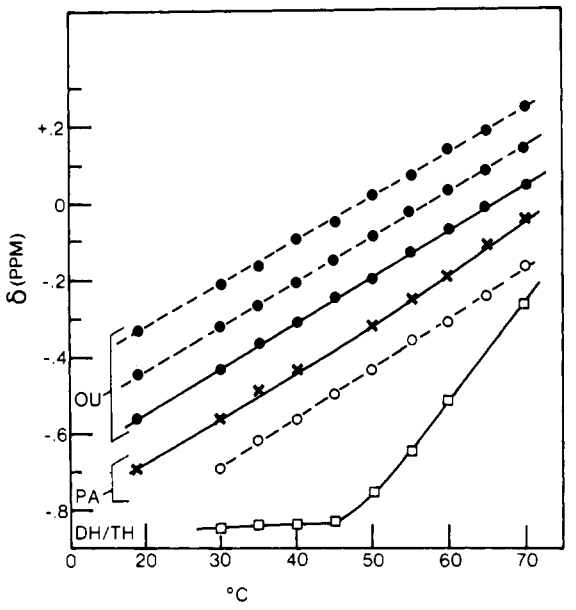

FIGURE 7: ^{31}P chemical shift vs. temperature for spectra of Figure 5B. Oligo(U) (●), poly(A) (×; ○), and multistrand helix (□). ^{31}P shifts for minor signals (●; ○) are shown as dashed curves.

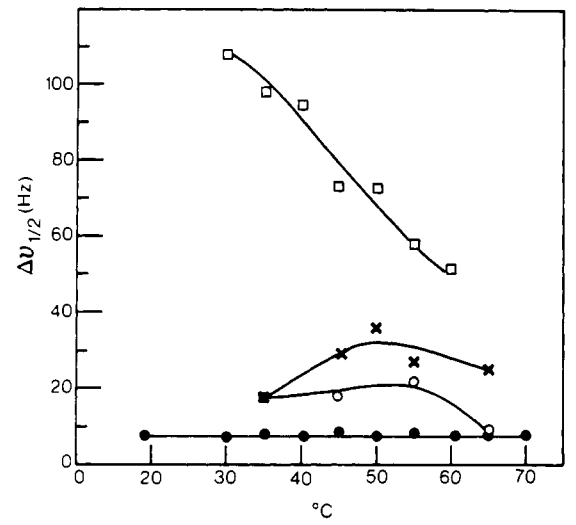

FIGURE 8: Plot of the corrected line widths of half-height ($\Delta\nu_{1/2}$) poly(A)-oligo(U) (1:2) spectra of Figure 5B (145.8 MHz). Oligo(U) signal (●), poly(A) signals (×; ○), and multistrand helix signal (□).

The polymeric multistranded helicle will be much more rigid than the poly(A) single helix, and the rotational motion of the molecule will be greatly reduced. This shortens the ^{31}P transverse relaxation time and broadens the signal. Thus Patel and Canuel (1976) observed only a very broad ^{13}P signal for the self-complementary poly[d(AT)] below 60 °C. The oligo(U)–poly(A) helix retains more flexibility than the polymer–polymer double helix and the ^{31}P signal for the former is not as broad. The oligo(U) will tumble even more rapidly than the poly(A) and therefore will have even narrower lines (and a longer T_1 as discussed earlier).

The frequency dependence to these line widths further supports the signal assignments. We have previously shown for tRNA^{Phe} that phosphorus relaxation is >90% dominated by the chemical shift anisotropy (CSA) mechainsm (Abragam, 1961) at 146 MHz while it is dominated by the dipole–dipole mechanism at lower field (Gorenstein & Luxon, 1979). The rotational correlation time for the tRNA^{Phe} and the poly(A)–oligo(U) multistrand helix will probably be similar, and hence the relaxation studies at high field will also likely be dominated by the chemical shift anisotropy mechanism. Recent relaxation studies on various double-helical systems confirm this suggestion (Bolton & James, 1980; Klevan et al., 1979). The CSA relaxation varies with the square of the magnetic field strength (Abragam, 1961) so that CSA broadening is expected to be 20× larger at 146 MHz as at 32 MHz ($146^2/32^2$). The presumed CSA contribution to the line width for the multistrand signal at 146 MHz is 50–109 Hz and will be $^1/_{20}$th or 2.5–4.2 Hz at 32 MHz. The 4–6-Hz residual broadening for this signal at the lower field is due to the dominant dipole–dipole relaxation mechanism (which is field-strength independent). Similar analysis explains the broadening of the poly(A) signal at higher field. The free oligo(U) signal is presumably dominated by the dipole–dipole term at both field strengths, consistent with the very short rotational correlation time for this molecule.

(2) The ^{31}P melting profiles (Figures 6 and 7) for the upfield signal show a sharp melting transition, characteristic of a cooperatively melting multistranded species. As shown earlier and seen for poly(A) or oligo(U) signals, the single-helix ^{31}P melting profiles are spread over a wider temperature interval, characteristic of a noncooperative, melting phenomenon. In

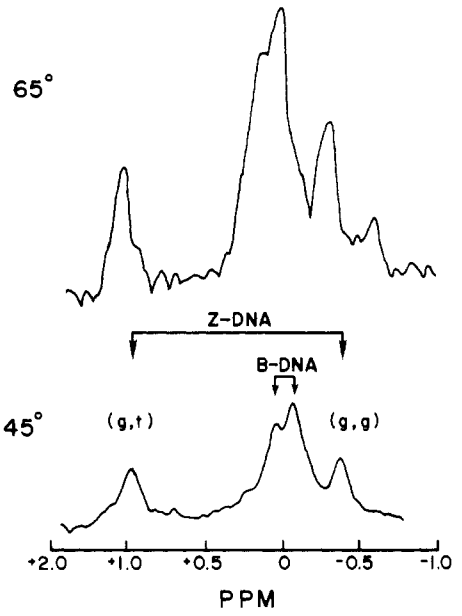

FIGURE 9: ^{31}P NMR spectra (32.4 MHz) of poly[d(GC)]·poly[d(GC)] (50 OD_{260} units/0.4 mL) in 4 M NaCl and 10 mM cacodylate, pH 7.0, at the indicated temperatures. 1-Hz exponential multiplication line broadening applied to 14 000–30 000 transients per spectrum.

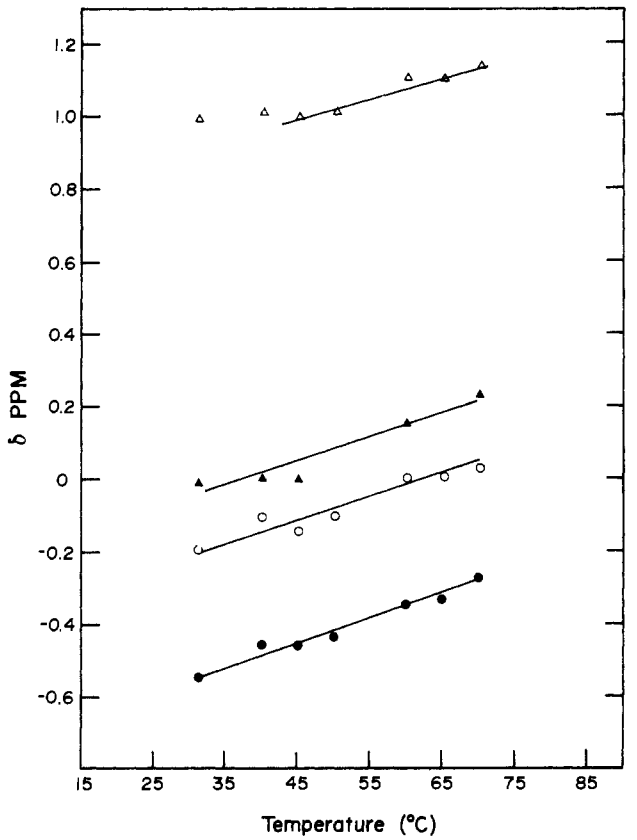

FIGURE 10: ^{31}P chemical shift vs. temperature for the signals of Figure 9.

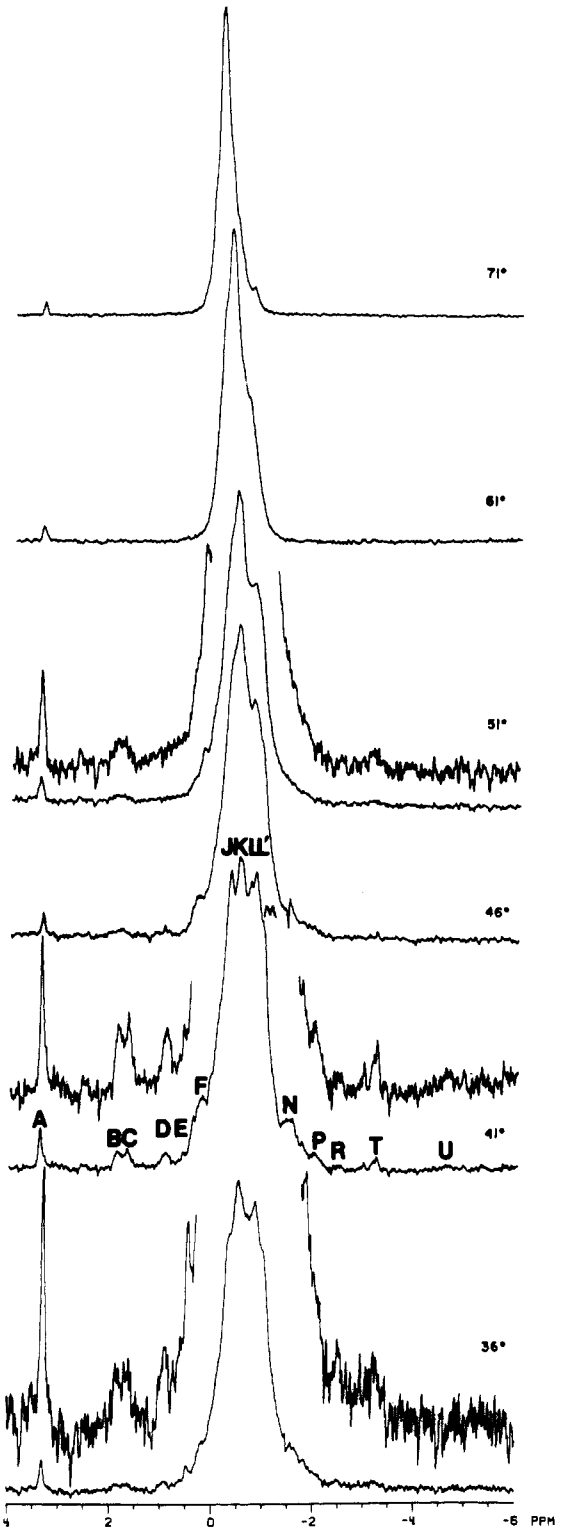

FIGURE 11: ^{31}P NMR spectra (145.8 MHz) of yeast $tRNA^{Phe}$ (33 mg/mL) in 100 mM NaCl, 10 mM cacodylate, and 1 mM EDTA, pH 7.0, at the indicated temperatures.

0.2 M NaCl, the melting temperature, T_m, for the poly(A)·U_{20} multistrand helix is 45–53 °C based upon the UV–VIS melting curves (Figure 2), the ^{31}P melting curves (Figures 6 and 7), or the temperature dependence to the integrated intensities for the poly(A)·oligo(U) helix. Below 35–40 °C in the 1:2 mixture in 0.2 M NaCl buffer solution, the upfield signal comprises 18 ± 4% of the total phosphate intensity. The multihelix signal intensity drops to near zero by 55 °C with $T_m \sim 48$ °C. In the 1:1 mixture, the signal intensity at 35 °C is 26% of the total and drops to zero by 55 °C with $T_m \sim 50$ °C. The low stability of the multistrand form is consistent with other spectrophotometric studies on oligo(U)·poly(A) mixtures (Lewis et al., 1975).

In order to ensure that there is no absolute loss of intensity at lower temperatures due to an unobservable, very broad signal, we also placed in several poly(A)·oligo(U) samples a concentric capillary of a trimethyl phosphate absolute standard in the NMR tube. At all temperatures the ratio of ^{31}P signal areas for trimethyl phosphate to nucleic acids was constant

(±2%), confirming that no ^{31}P signals are buried in the base line of Figures 4 and 5.

A more exact analysis of signal areas is not possible since in most spectra 90° pulses were not used and the pulsing recycle interval was 2 s, which is comparable to the ^{31}P T_1 relaxation times [see Results and Gorenstein & Luxon (1979), Klevan et al. (1979), and Bolton & James (1980)]. Longer relaxing species [such as the small molecule oligo(U) with T_1 of 3 s] will be partially relaxed, and the signal area will not exactly reflect nuclear populations. Recall that at 60 °C in Figure 4, the oligo(U) and poly(A) signal areas are not 1:1, partially due to this effect. In addition, at lower temperatures an unknown relative population of triple and double helices is present. In Figure 5A at 45 °C, the poly(A) single-strand signal is considerably larger than the oligo(U) single-strand signal, suggesting that more of the oligo(U) than the poly(A) phosphates contribute to the upfield multistrand ^{31}P signal. This confirms that a triple helix is indeed present. Apparently both poly(A) and oligo(U), locked into *g,g*, helical conformations of the multistrand species, contribute to this upfield signal since no splitting of the multihelix signal is observed. In addition, both double and triple helices must give similar ^{31}P chemical shifts (both *g,g* conformations).

^{31}P Spectra of Poly[d(GC)]·Poly[d(GC)]. There has been considerable recent interest in the high-salt form of poly[d(GC)]·poly[d(GC)] (Pohl & Jovin, 1972) because of its unusual Z-DNA conformation. It has been spectulated that this new conformation has some biological significance (Wang et al., 1979, 1981; Drew et al., 1980), and it is very interesting that the unique ^{31}P NMR features of Z-DNA are similar to those of various drug–duplex DNA or RNA complexes (Patel, 1979; Reinhardt & Krugh, 1977; Gorenstein, 1981). X-ray crystallographic analysis of small d(GC) oligomers (Wang et al., 1979, 1981; Drew et al., 1980; Crawford et al., 1980) and ^{31}P NMR analysis of $d(GC)_{8-11}$ (Patel et al., 1979), 145-bp poly[d(GC)] (Simpson & Shindo, 1980), poly[d(GC)]·poly[d(GC)] (Patel, 1979b), and sonicated polymer samples [50–200 bp in length (Cohen et al., 1981)] have indicated that under certain crystallizing conditions or high salt solution conditions, a new left-handed duplex form is stabilized. One of the unusual distinguishing characteristics of this Z-DNA conformation is that the phosphate ester torsional angle alternates between *g,g* and *g,t* along the duplex strands while in normal B-DNA the P–O ester conformation is uniformly *−g,−g*. As pointed out in the earlier ^{31}P NMR studies, the appearance of two nearly equal ^{31}P signals separated by 1.4–1.5 ppm is likely a reflection of the two different P–O ester conformations, as observed in the crystalline state.

We had earlier predicted based upon ^{31}P chemical shift calculations and various model system studies that the ^{31}P chemical shift of a *g,t* phosphate diester should be 1.4 ppm downfield from the B-DNA *g,g* conformation (Gorenstein & Kar, 1975; Gorenstein & Luxon, 1979; Gorenstein, 1981). There can be little doubt that poly[d(GC)]·poly[d(GC)] in high-salt (4 M NaCl) solution exists in the Z-DNA conformation and that the downfield signal originates from phosphate diesters in *g,t* conformations. Spectra in Figure 9 are qualitatively similar to that reported by Patel (1979b) for poly[d(GC)]·poly[d(GC)] except that he observed two peaks separated by 1.4 ppm of unequal area (the downfield signal being smaller than a broader upfield signal). His spectrum was taken at 145.7 MHz and 80.5 °C, and the signals are considerably broader (50–100-Hz line widths) than those of Figure 9 (~7-Hz line width). As explained above, the larger line width is expected at higher field due to the frequency dependence of the chemical shift anisotropy relaxation mechanism. With the better resolution obtainable at lower field, we can actually identify four different signals in the ^{31}P spectra shown in Figure 9. Besides the two Z-DNA signals, two larger, approximately equal signals at 0 and −0.14 ppm (45 °C) are assigned to normal right-handed, B-DNA phosphates. Thus, a small conformational difference also must exist even between the two phosphates of the B-DNA in this sample. Similar small separations have been noted previously (Gorenstein, 1981; Patel, 1979a,b; Cohen et al., 1981).

Klysik et al. (1981) have shown that a section of right-handed B-structure DNA can coexist with the left-handed Z-DNA structure in a 157-bp restriction fragment containing a 95-bp *lac* fragment flanked by d(GC) sequences. In their ^{31}P NMR spectrum in 5.0 M NaCl, a smaller signal representing ~20% of the total phosphate is 1.45 ppm downfield from the larger and broader upfield signal [similar to Patel's (1979b) spectrum]. Since the DNA fragment contains 37% d(GC) tracts, essentially all the d(GC) is in the Z-DNA conformation (20% *g,g* + 20% *g,t*). Our ^{31}P NMR results shown in Figure 4B confirms that the increased width of their upfield signal is surely due to a noncoincident superposition of B-DNA *g,g* phosphate and Z-DNA *g,g* phosphate signals. As pointed out by Klysik et al. (1981), the biological (i.e., regulatory) implications of the possible coexistence of B and Z helices in DNA may be profound.

Finally, it should be noted that $d(GC)_4$ (Collaborative Research) does *not* form the Z-DNA structure at 4–5 M NaCl (when the ^{31}P NMR spectrum criterion is used since no downfield *g,t* ^{31}P signals could be found). This suggests that for shorter oligomers (4–8 bp) Z-DNA requires a d(CG) rather than a d(GC) repeat. Significantly, only short oligomers of the sequence d(CG) have been shown to form Z-DNA structures in X-ray crystallographic studies. Drew et al. (1981) have shown that the DNA dodecamer d(CGCGAATTCGCG) forms a B-DNA double helix in spite of the tetrameric d(CGCG) ends which might be expected to form short tracts of Z-DNA attached to a d(AATT) B-DNA section. This results is still consistent with the work of Klysik et al. (1981), who showed in their 157 base pair fragment that a junction of ~11 bp exist between the purely B-DNA and Z-DNA tracts. Their CD results suggest that this 11-bp d(GC) junction does not have the Z-DNA glycosidic bond conformation (G residues are syn in Z-DNA but anti in B-DNA). However, their ^{31}P NMR results showing essentially all d(GpC) phosphates in *g,t* conformations suggest that this junction region does have phosphates in the *g,t* P–O ester bond Z-DNA conformation. Significantly, in Drew et al. (1981) the O3′–P torsional angles for C_1, G_4, G_{10}, and G_{22} are trans (all others as all P–O5′ angles are gauche). Thus it would appear that a phosphate in a *g,t* conformation is a necessary but *not* sufficient condition for formation of the Z-DNA structure.

Transfer RNA ^{31}P NMR Spectra. The ^{31}P NMR spectra for yeast $tRNA^{Phe}$ supports the assignments of the *g,g* phosphates to the upfield signal in Figures 4 and 5. The upfield signal in the main cluster (signal M in Figures 11 and 12) has been rather unambiguously assigned to the double-helix diester phosphates (Gueron & Shulman, 1975; Gorenstein & Luxon, 1979; Salemink et al., 1979, 1981; Gorenstein et al., 1981). Thus, in the 10 mM Mg^{2+} ^{31}P spectra signals L and M integrate for 35 phosphates and in the X-ray structure 32 phosphates (largely in the double-helical stem regions of the molecule) are in a gauche,gauche conformation. As shown in Figure 12, the ^{31}P chemical shift changes of peak M in the

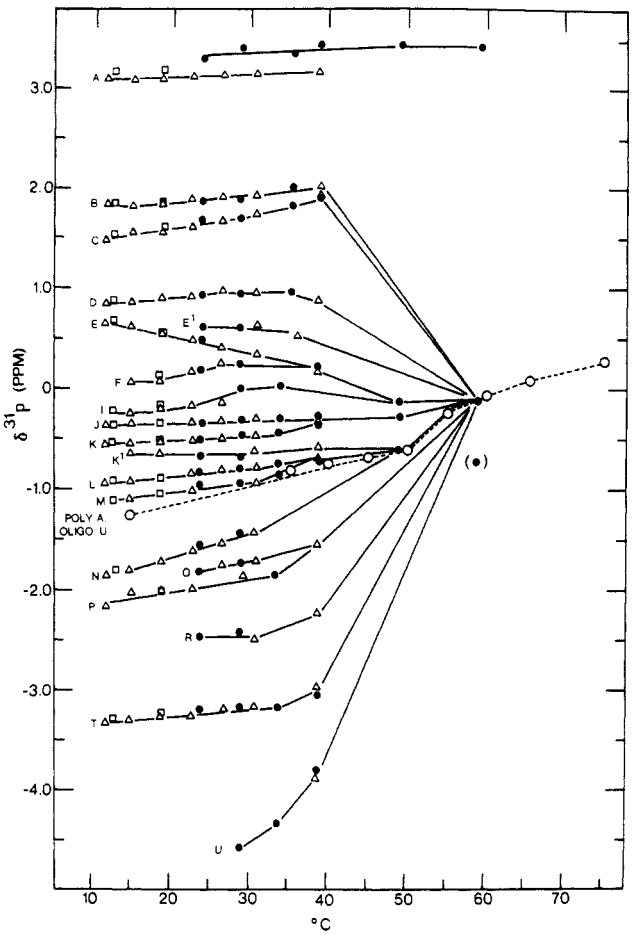

FIGURE 12: Temperature dependence to the chemical shifts, δ, of the indicated peaks from Figure 11 at 145.8 MHz. (●), (△), and (□) represent different samples. Also, the ^{31}P shift of the multihelix signal (○) of poly(A)·oligo(U) (1:1) is reproduced from Figure 6.

0.2 M NaCl (no Mg^{2+}) $tRNA^{Phe}$ sample are very similar to changes in the upfield (multistrand) signal in the poly(A)·oligo(U) complex. The similarity in the melting transition (T_m's ~ 48 °C) is largely coincidental though the disruption of 20 A·U (or A·U·U) bp or triplets in poly(A)·oligo(U) is probably similar energetically to the melting of the four stems with 20 bp in native tRNA.

The $tRNA^{Phe}$ scattered signals B–F and S–U arise from the tertiary structure and integrate for less than one phosphate each at 36 °C, and excess intensity (five phosphates) appears in the spectral region corresponding to nonhelical, "random coil" phosphates (–0.7 to 0 ppm; a shoulder to peak K). These spectral differences are largely due to partial melting of the native structure, as further shown by the changes in the ^{31}P spectra at higher temperature.

Significantly, these scattered signals and main cluster signals shift very little (<0.2 ppm) prior to breakup of the secondary and tertiary structure. This is consistent with the overall constancy of the tRNA structure below T_m. The torsional angles are more rigidly constrained to fixed values in the native tRNA, and thus the ^{31}P signals shift little with temperature prior to disruption of this structure. In contrast, even below the poly(A)·oligo(U) T_m there is still a sizable further upfield shift with decreasing temperature (Figure 5A). This is likely a real shift representing an increase in the population of *g,g* structures in the double and triple helices due to chemical exchange effects (see below). The incomplete leveling in the UV melting curves below T_m (Figure 2) also suggests more ordered structures (stacked, single helices) are formed at lower temperatures. The observation that only 20–26% of the phosphates are in double or triple helices confirms that a large percentage of the complementary nucleic acid mixture in these samples is in single helix and random coil states throughout the temperature range from 5 to 85 °C.

Kinetics. To our knowledge these ^{31}P NMR studies represent the first time separate NMR signals for the multistrand state and single-strand state have been observed. For this to be possible, chemical exchange of the nucleic acid components between the single and multistrand states must be slow on the NMR time scale, or

$$\tau > 1/(2\pi\Delta\nu)$$

where τ is the lifetime of the exchanging nuclei and $\Delta\nu$ is the chemical shift difference in hertz between the two states. Since $\Delta\nu \sim 20$ Hz (at 32 MHz) for the poly(A)–oligo(U) single to multistrand exchange, $\tau \geq 8$ ms. Greslauer et al. (1975) have observed a relaxation time $\tau \sim 14$ ms at 35 °C for the melting of double-stranded A_7U_7 in 1 M NaCl. At lower temperatures the lifetime of the double helix will be even longer. In addition, the longer chain length for the oligo(U) strand also increase τ (Craig et al., 1971; Porschke & Eigen, 1971; Porschke, 1971). This estimate of the lifetimes for these states suggests we should be in the slow exchange limit, which is consistent with the observation of two signals (Pople et al., 1959). Note that at 146 MHz with $\Delta\nu \sim 70$ Hz we should certainly be in the slow exchange limit at lower temperature. This is confirmed by the temperature dependence to the ^{31}P line width for poly(A) at 145.8 MHz (Figure 8). The line widths for the poly(A) signals reach a maximum at $T_m \sim 50$ °C. This behavior suggests that chemical exchange line broadening contributes to the line width of the poly(A) signals. Note also that the ^{31}P chemical shift–melting curves of the poly(A) and oligo(U) single strands at 145.8 MHz do not show an inflecton point at $T_m \sim 50$ °C (Figure 7), whereas an inflection point is observed in the ^{31}P chemical shift–melting curves of the single-strand poly(A) at 32.4 MHz (Figure 6). At the higher field, below T_m, the single-strand and multistrand forms are in slow to intermediate chemical exchange. Line widths are affected but chemical shifts are not (Pople et al., 1959), so that the chemical shift of the multihelix signal below 45 °C at 145.8 MHz does not shift with temperature (Figure 7). At lower field, around T_m the poly(A) and multistrand forms are in intermediate to fast chemical exchange so that the poly(A) single-strand ^{31}P signal shifts further upfield as the temperature is lowered through the T_m: some multihelix state is averaged into the single-strand state. It is not possible to describe the relative populations (and ^{31}P signal areas) for single- and multistrand states at intermediate temperatures, 32.4 MHz, because of this chemical exchange averaging and the difficulty described above for quantification of signal areas.

At lower temperatures chemical exchange is slow enough to allow signal areas to directly reflect strand populations (especially if recycle times greater than five T_1's are used). Under these conditions ^{31}P NMR will allow facile estimation of the fraction of multistrand vs. single-strand states by direct integration of the separate signals.

Acknowledgments

The contribution to this work by Vickie Bowie and Rouhlwai Chen is acknowledged.

References

Abragam, A. (1961) *The Principles of Nuclear Magnetism*, Oxford University Press, New York.

Akasaka, K. (1975) *Biopolymers 13*, 2273.

Akasaka, K., Yamada, A., & Hatano, H. (1975) *FEBS Lett. 53*, 339.
Arnott, S. (1970) *Prog. Biophys. Mol. Biol. 21*, 267.
Bloomfield, V. A., Crothers, D. M., & Tinoco, I. (1974) *Physical Chemistry of Nucleic Acids*, Chapter 6, Harper & Row, New York.
Bolton, P. H., & James, T. L. (1980) *Biochemistry 19*, 1388.
Borer, P. N., Kan, L. S., & Ts'o, P. O. P. (1975) *Biochemistry 14*, 4847.
Breslauer, K. J., Sturtevant, J. M., & Tinoco, I. (1975) *J. Mol. Biol. 99*, 549.
Cohen, J. S., Wooten, J. B., & Chatterjee, C. C. (1981) *Biochemistry 20*, 3049.
Cozzone, P., & Jardetzky, O. (1976) *Biochemistry 15*, 4853.
Craig, M. E., Crothers, P. M., & Doty, P. (1971) *J. Mol. Biol. 62*, 383.
Crawford, J. L., Kolpak, F. J., Wang, A. H.-J., Quigley, G. J., van Boom, J. H., van der Marel, G., & Rich, A. (1980) *Proc. Natl. Acad. Sci. U.S.A. 77*, 4016.
Drew, H., Takano, T., Tanaka, S., Itakura, K., & Dickerson, R. E. (1980) *Nature (London) 286*, 567.
Drew, H. R., Wing, R. M., Takano, T., Broka, C., Tanaka, S., Itakura, K., Dickerson, R. E. (1981) *Proc. Natl. Acad. Sci. U.S.A. 78*, 2179.
Gorenstein, D. G. (1975) *J. Am. Chem. Soc. 97*, 898.
Gorenstein, D. G. (1978) *Jerusalem Symp. Quantum Chem. Biochem. 11*, 1.
Gorenstein, D. G. (1981) *Annu. Rev. Biophys. Bioeng. 10*, 355.
Gorenstein, D. G., & Kar, D. (1975) *Biochem. Biophys. Res. Commun. 65*, 1073.
Gorenstein, D. G., & Luxon, B. A. (1979) *Biochemistry 18*, 3796.
Gorenstein, D. G., Findlay, J. B., Momii, R. K., Luxon, B. A., & Kar, D. (1976) *Biochemistry 15*, 3796.
Gorenstein, D. G., Goldfield, Chen, R., Kovar, K., & Luxon, B. A. (1981) *Biochemistry 20*, 2141.
Gueron, M., & Shulman, R. G. (1975) *Proc. Natl. Acad. Sci. U.S.A. 72*, 3482.
Haasnoot, C. A. G., & Altona, C. (1979) *Nucleic Acids Res. 6*, 1135.
Hanlon, S., Glonek, T., & Chan, A. (1976) *Biochemistry 15*, 3869.
Kan, L. S., Ts'o, P. O. P., Sprinzl, M., van der Haar, F., & Cramer, F. (1977) *Biochemistry 16*, 3143.
Kim, S. H., Berman, H. M., Seeman, N. C., & Newton, M. D. (1973) *Acta Crystallogr., Sect. B 29*, 703.
Klevan, L., Armitage, Ian, M., & Crothers, D. M. (1979) *Nucleic Acids Res. 6*, 1607.
Klysik, J., Stirdivant, S. M., Larson, J. E., Hart, P. A., & Wells, R. D. (1981) *Nature (London) 290*, 672.
Lewis, J. B., Brass, L. F., & Doty, P. (1975) *Biochemistry 14*, 3164.
Patel, D. J. (1979a) *Acc. Chem. Res. 12*, 118.
Patel, D. J. (1979b) in *Stereodynamics of Molecular Systems*, pp 397–422, Pergamon Press, New York.
Patel, D. J., & Canuel, L. (1976) *Proc. Natl. Acad. Sci. U.S.A. 73*, 674.
Patel, D. J., Canuel, L. L., & Pohl, F. M. (1979) *Proc. Natl. Acad. Sci. U.S.A. 76*, 2508.
Pohl, F. M., & Jovin, T. M. (1972) *J. Mol. Biol. 67*, 375.
Pople, J. A., Schneider, W. G., & Bernstein, H. J. (1959) *High Resolution Nuclear Magnetic Resonance*, Chapters 9 and 10, McGraw-Hill, New York.
Porschke, D. (1971) *Biopolymers 10*, 1989.
Porschke, D., & Eigen, M. (1971) *J. Mol. Biol. 62*, 361.
Pradd, F. R., Giessner-Prettre, C., Pullman, B., & Daudex, J.-P. (1979) *J. Am. Chem. Soc. 101*, 1737.
Reinhardt, C. G., & Krugh, T. R. (1977) *Biochemistry 16*, 2890.
Robillard, G. T., Tarr, C. E., Vosman, F., & Reid, B. R. (1977) *Biochemistry 16*, 5261.
Romer, R., Riesner, D., Maass, G., Wintermeyer, W., Thiebe, R. & Zachau, H. G. (1969) *FEBS Lett. 5*, 15.
Salemink, P. J. M., Swarthof, T., & Hibers, C. W. (1979) *Biochemistry 18*, 3477.
Salemink, P. J. M., Reijerse, E. J., Mollevanger, L. C. P. J., & Hilbers, C. W. (1981) *Eur. J. Biochem. 115*, 635.
Simpson, R. T., & Shindo, H. (1980) *Nucleic Acids Res. 8*, 2093.
Stevens, C. L., & Felsenfeld, G. (1964) *Biopolymers 2*, 293.
Sundaralingam, M. (1969) *Biopolymers 7*, 821.
Ts'o, P. O. P. (1975) *Basic Principles in Nucleic Acid Chemistry*, Vol. I and II, Academic Press, New York and London.
Wang, A. H.-J., Quigley, G. J., Kolpak, F. J., Crawford, J. L., Van Boon, J. H., Van der Marel, G., & Rich, A. (1979) *Nature (London) 282*, 680.
Wang, A. H.-J., Quigley, G. J., Kolpak, F. J., Van der Marel, G., Van Boon, J. H., & Rich, A. (1981) *Science (Washington, D.C.) 211*, 171.
Yamada, A., Kaneko, H., Akasaka, K., & Hatano, H. (1978) *FEBS Lett. 93*, 16.